ever, it is a more accurate method, with simpler derivation of the boundary conditions, than method II. Nevertheless, such simple representations of derivatives in the finite element method are limited to square, cubic or rectangular elements.

C. Numerical Result

1. *Hunt's example*

We used Hunt's example of a 4 × 6 element rectangle to check the programming of the Hunt's method. The results are in complete agreement with the published results.

2. *Square domain*

The results of the three methods applied to a square domain are given in Table 1. It can be seen that the finite element method based on ϕ using the central differences and the central averages is the most accurate, and also it is the simplest to program. Method III is faster than method II because the matrix inversion has been accomplished by breaking down the matrix to smaller submatrices and inverting one row at a time from the bottom up,† noting that the matrix inversion time for a medium size matrix is proportional to n^3. Method I for an 11 × 11 domain takes a very long machine time because of the apparent necessity to use disk storage outside the computer core, due to the presence of a large augmented matrix. Further, the long CP (Central Processor) time is due to the large eigenvalue problem that arises unless Hunt's intuitive method of eliminating the zero frequency modes is used.‡ For the latter, CP time could be greatly reduced while PP (Peripheral Processor) time would be further increased. Methods II and III have a steady motion mode which was excluded, and the 9th and 10th modes in the 11 × 11 case should not be taken seriously since these are the last two modes.

D. Conclusion

The finite element method based on the velocity potential ϕ with the central differences and the central averages is the most efficient of the three methods compared. However, a square, a cubic, or a rectangular domain is required before the central differences and the central averages can be applied. Since simple finite difference methods may be less accurate, it appears that a "machine transformation"§[5] combined with variational principles may be the most efficient for three-dimensional sloshing. It is noted that this approach may be comparable with the Khabbaz' method.[6] However, the quadrature formula given in Ref. 6 may not be optimum. Even for the first mode, the numerical value of the natural frequency undershoots the exact value as the mesh is refined. It is doubtful that the undershooting is due to round-off errors; it is probably a truncation error, the solution of which may not approach the exact solution in the limit. The proposed approach would be approximately a second-order process, provided that suitable mapping is employed.

References

[1] Zienkiewicz, A. C. and Cheung, Y. K., "The Finite Element Method in Structures and Continuum Mechanics," McGraw-Hill, New York, 1967.

[2] Hunt, D. A., "Discrete Element Structure Theory of Fluids," AIAA Paper 70-23, New York, 1970.

[3] Emery, A. F. and Carson, W. W., "Evaluation of Use of the Finite Element Method in Computation of Temperature," ASME Paper 69 WA/HT38, Nov. 16–20, 1969, Los Angeles, Calif..

[4] Milne, W. E., "Numerical Solution of Differential Equations," Wiley, New York, 1953, p. 131.

† In method II, two-step inversion is used.

‡ This was used in the 6 × 6 case.

§ An abbreviated term for the numerical transformation using high speed computer.

[5] Chu, W. H., "Development of General Finite Difference Approximation for a General Domain, Part I—Machine Transformation," SwRI Project IR 02-9034-01, Final Rept., Aug. 1970, *Journal Computational Physics*, to be published.

[6] Khabbaz, G. R., "Dynamic Behavior of Liquids in Elastic Tanks," LMSC 60-80-70-23, Aug. 1970, Lockheed Missiles & Space Co., Palo Alto, Calif.

A Higher Performance Electric-Arc-Driven Shock Tube

WESLEY A. MENARD
Jet Propulsion Laboratory, Pasadena, Calif.

Introduction

SIMULATION of Jupiter and Saturn atmospheric entry has been difficult[1] because entry velocities range from 25–48 km/sec. Shock tube velocities have been limited to about 15 km/sec.[2–4] The purpose of this Note is to report the development of an electric arc-driven shock tube which has increased shock velocity by a factor of three. The new driver has a conical internal design of small volume, and uses lightweight diaphragms. Data obtained from a 15.2-cm-diam driven tube show little shock wave attenuation. Shock velocities of 45 km/sec with test times in excess of 4 μ sec have been attained.

Shock Tube

Energy for the driver is supplied by a 100 capacitor storage system, rated at 290,000 joules when charged to 20,000 v. The new driver is shown schematically in Fig. 1 and is a modification of an earlier design.[5] The cathode is a 3.2-cm-diam cylinder made from Mallory 1000 (a sintered tungsten alloy). A hole in the cathode tip allows for pulling through the trigger wire. The anode is a 2.5-cm-wide, 7.7-cm-diam copper ring located 9.6 cm from the cathode. A conical teflon insert reduces the driver volume to 350 cm^3, and provides a fairly smooth internal contour from the cathode tip to the 15.2-cm-diam driven tube. The diaphragm is located on the downstream side of the anode ring. A 0.025-cm-diam stainless steel wire is strung across the opening, and attached to this wire is the trigger pull wire. In operation, pulling the trigger wire toward the cathode initiates the arc.

Mylar diaphragms (0.35 mm thick) are used to reduce diaphragm opening losses and to insure a fast opening time. Helium or hydrogen gas is supplied to the driver at a pressure (11.8 atm) 4% less than the static rupture pressure of the diaphragms. When the arc is struck, the trigger wires and the diaphragm immediately disintegrate. At high driver energies the copper anode could not hold the arc. Severe erosion on the surface of the stainless steel transition section indicated the arc had extended 7 cm beyond the diaphragm. Current measurements of the capacitor bank discharge show the arc burns for about 25 μsec. The driver gas can receive energy from the arc while in the driver, and as it expands down the tube.

Measurements

The most abundant elements in the atmospheres of Jupiter and Saturn are believed to be hydrogen and helium. For this reason the majority of shock tube runs were made in a mixture of 80% He and 20% H_2 (by volume).

Received April 28, 1971.
This research sponsored by NASA under contract NAS 7-100.

* Senior Research Engineer. Member AIAA.

Table 1 Shock velocity, test time, and equilibrium temperature for several driver and driven gages, measured at two distances from the diaphragm[a]

Driven Gas	Helium Driver Gas		Hydrogen Driver Gas		Temperature °K (for vel*)
	3.66m	10.67m	3.66m	10.67m	
Hydrogen	...	...	45.0* (4–7)	39.5 (6)	12,300
0.2 H_2–0.8 He	30.8 (5)	28.4 (7)	41.3* (4)	40.4 (6)	22,000
Helium	34.4* (4)	28.9 (6)	...	...	21,000
Air	27.9* (7)	23.1 (11)	32.7 ...	20.3 (11)	31,000
Argon	25.7 ...	20.0* (12)	31.7 ...	15.8 (12)	34,700

[a] Shock velocity in km/sec, test time (in parenthesis) in μsec. Initial driven gas pressure = 0.05 torr. Capacitor bank energy = 2.9 × 10^5 joules.

Shock velocities were measured with collimated photomultipliers. Data obtained in 0.25 torr of the test gas, over a range of driver energies are presented in Fig. 1. The driver gas is helium, and the data were taken at 3.66 and 10.67 m from the diaphragm. Velocities ranging from 12 to over 32 km/sec were obtained. The velocity increases continuously as energy is increased with no indication of leveling off. This result appears to indicate that even higher speeds could be reached if more energy were available. The effect of initial pressure on performance was studied by varying the test gas pressure from 50–0.05 torr while holding energy constant. Shock velocities from 10–32 km/sec were measured. Attenuation of the shock wave over a distance of 7 m was 10% at the lowest pressures, increasing to 35% at 50 torr.

Runs were also made in pure hydrogen, helium, air and argon, using helium and hydrogen driver gases. A summary of results is presented in Table 1. Shock velocity and test time data at two tube locations are given. The test times, in μsec, are in parenthesis. With a helium driver shock speeds in the lightweight gases are greater than 30 km/sec, and in the heavy gases, $U_s \geq 20$ km/sec. A further increase in shock velocity is obtained when hydrogen is used as the driver gas. Hydrogen driven shock waves as fast as 45 km/sec have been produced.

The final column in Table 1 shows the equilibrium temperatures calculated[6] for the asterisk (*) data. These temperatures are extremely high for incident shock waves. In fact, comparable temperatures have not been produced in the reflected waves of other conventional shock tubes.

Three types of measurements were made to determine test times: 1) wide band pass radiation measurements from the sidewall; 2) narrow band pass measurements from the sidewall; and 3) heat-transfer measurements on a model located on the tube centerline. Wide band radiation was observed with a collimated photomultiplier having an S-11 (visible) response. The narrow band measurements were made with a photomultiplier viewing the gas through a 50 Å half-width, narrow band pass filter. The center wavelength was selected to coincide with the intense H_α line (6563 Å). As the test slug passed the viewing station radiation from hydrogen would disappear upon arrival of the helium driver gas. Two calorimeter heat-transfer measurements were made to verify the results from the radiation techniques. Both measurements showed a linear slope of the output which is typical of constant stagnation point heating. The temperature change at the contact surface was recorded as an abrupt voltage change in the gauge output.

For all the gases tested the measured test time could be correlated to the time r/a_2, where r is the tube radius and a_2 is the speed of sound in the shock heated gas. The correlation was better than ±50% when $U_s \geq 18$ km/sec and $P_1 \leq 1$ torr.

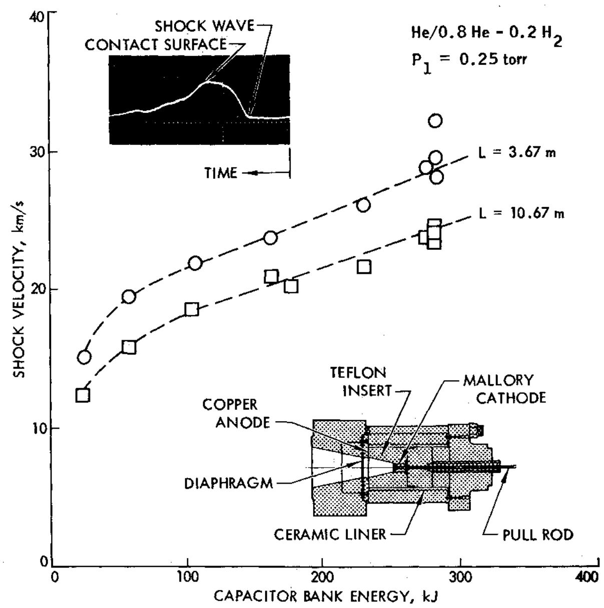

Fig. 1 Variation in shock velocity with energy input for the conical driver. Oscillograph record shows H_α line intensity for a 26.5 km/sec shock wave.

A comparison with performance from other shock tubes is made in Fig. 2. The JPL results are plotted for air and the 0.2 H_2–0.8 He mixture at P_1 = 0.05 torr. The other techniques used air at pressures ranging from 0.05–10.0 torr.[2,3] The new velocities exceed all other driving techniques except the electromagnetic driver, and the modest attenuation is comparable to the combustion, piston, electrical, and two of the implosion drivers.

Conclusions

The driver described in this note has significantly increased performance of the electric-arc-driven shock tube. By adding energy to an expanding driver gas, shock velocities as high as 45 km/sec have been achieved. Attenuation of the shock wave was small for most experimental conditions, and test times greater than 4 μsec were measured. Shock speeds capable of simulating outer-planet entry have been demonstrated, and the measurements of Fig. 1 imply higher velocities would be possible if more energy were available.

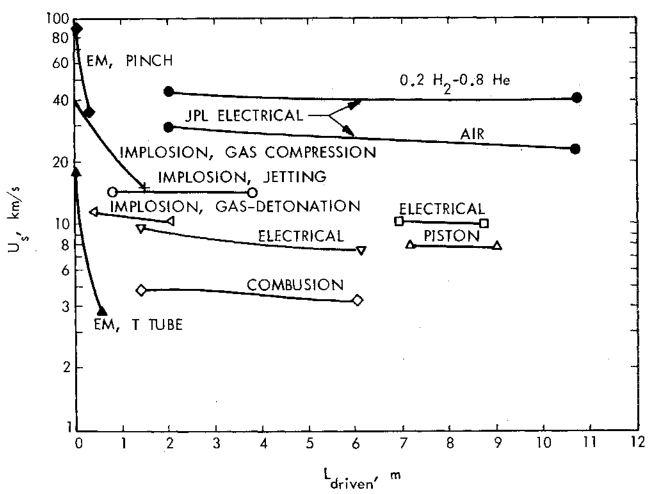

Fig. 2 Comparison of present JPL performance with other driving techniques.[2,3]

References

[1] Menard, W. A. and Stickford, G. H., "Shock Tube Measurements of Radiation from a Simulated Jupiter Atmosphere," AIAA Paper 69-184, New York, 1969.

[2] Glass, I. I., "Appraisal of UTIAS Implosion-Driven Hypervelocity Launchers and Shock Tubes," UTIAS Review 31, June 1970, Inst. for Aerospace Studies, Univ. of Toronto, Canada.

[3] Warren, W. R. and Harris, C. J., "A Critique of High-Performance Shock Tube Driving Techniques," *Shock Tubes, Proceedings of the Seventh International Shock Tube Symposium*, University of Toronto Press, 1970, pp. 143–176.

[4] Dannenberg, R. E., "An Imploding Trigger Technique for Improved Operation of Electric Arc Drivers," *Shock Tubes, Proceedings of the Seventh International Shock Tube Symposium*, University of Toronto Press, 1970, pp. 186–200.

[5] Williard, J. W., "Performance of a Ceramic-Lined-6-In.-Diameter Arc Driver," AIAA Paper 68-366, San Francisco, Calif., 1968.

[6] Menard, W. A. and Horton, T. E., "Shock Tube Thermochemistry Tables for High Temperature Gases, Vol. I, Air, and Vol. III, Helium, Neon, and Argon," TR 32-1408, Vol. I, Nov. 1969; also Vol. III, Jan. 1970, Jet Propulsion Lab., Pasadena, Calif.

Koiter's Modified Energy Functional for Circular Cylindrical Shells

C. P. Mangelsdorf*

University of Pittsburgh, Pittsburgh, Pa.

Nomenclature

E	= modulus of elasticity of shell material
h	= shell thickness
R	= shell radius
u,v,w	= shell displacements in longitudinal, circumferential and radial directions, respectively
$(\ )',(\ )^{\cdot}$	= derivatives of displacements with respect to longitudinal or circumferential coordinates, respectively
ν	= Poisson's ratio
dS	= infinitesimal element of shell middle surface

Introduction

THE search for simple and convenient yet accurate equations to describe the behavior of circular cylindrical shells led Donnell[1] to make approximations which Hoff[2] has shown limit the accuracy of Donnell's equations to relatively short shells. Seeking equations of more general value, Morley[3] proposed but did not rigorously justify a modification of the Donnell equations which appeared to preserve the convenience of the originals while possessing an accuracy comparable to Flügge's[4] over a broad range of practical shell proportions. Now Koiter has suggested a rational modification to his energy functional[5] which yields, by way of variational methods, equilibrium equations which, in turn, can be reduced by substitution and successive derivatives to Morley's modified form of Donnell's equations. The purpose of this Note is to report the basis and form of Koiter's modified energy functional.

Modified Energy Functional

For a circular cylindrical shell of radius R and uniform thickness h, the strain energy for small finite deflections as given by Koiter[5] is

$$P_2[\mathbf{u}] = \int \{[Eh/2(1-\nu^2)R^2][u'^2 + (v^{\cdot} + w)^2 + 2\nu u'(v^{\cdot} + w) + \tfrac{1}{2}(1-\nu)(u^{\cdot} + v')^2] + \quad \text{(line 1)}$$

$$+ [Eh/24(1-\nu^2)R^4][w''^2 + (w^{\cdot\cdot} - v^{\cdot})^2 + 2\nu w''(w^{\cdot\cdot} - v^{\cdot}) + 2(1-\nu)(w' + \tfrac{1}{4}u^{\cdot} - \tfrac{3}{4}v')^2]\}dS \quad (1) \quad \text{(line 2)}$$

where $\mathbf{u}$ is a generalized displacement field and the actual displacements and their derivatives are defined in the Nomenclature. In view of the length and complexity of this expression and the influence it exerts upon subsequent expressions which can be generated from it by variational techniques, there is some desirability in introducing modifications which will lead to the ultimate solution of any particular problem with a minimum of effort. Such modifications can be accomplished by the addition or subtraction of negligibly small terms, provided a proper basis for negligibility can be established.

In general, the only such basis would be the sum of all the terms in the expression. To say that any term is negligible because it is small compared to some other term overlooks the possibility that there may be yet other terms containing the same displacement derivatives as, of the same order of magnitude as, and of opposite sign from, that term used for comparison. When combined, these larger terms could produce a sum which was not much larger than the term one is trying to show is negligible.

However, since Eq. (1) is a strain energy expression for which the sum of all the terms must be positive for stable equilibrium, it is possible to subdivide the expression into groups of terms, the sums of which are, by themselves, positive. The first such subdivision would naturally be lines 1 and 2 taken separately since they represent strain energy due to membrane and bending action, respectively. It will further be noted that the first three terms in both lines 1 and 2 are of the form

$$b^2 + 2\nu bc + c^2 \qquad (2)$$

which must be positive irrespective of the values of b and c (as long as ν is less than 1). The remaining term in each line must also be positive since it is a squared term. We now have four independent bases for establishing the negligibility of terms.

For example, a term such as $[Eh^3/24(1-\nu^2)R^4](u^{\cdot} + v')^2$ can be compared to the last term of line 1 and found to be in the ratio $h^2/6(1-\nu)R^2$, which for thin shells may properly be taken as negligible. On the other hand, the negligibility of a term containing v'^2, by itself, could not be determined because no usable basis for comparison is available.

As another example, a term such as $[Eh^3/24(1-\nu^2)R^4](v^{\cdot} + w)^2$ must be compared to the sum of the first three terms of line 1, leading to a ratio of the type $(h^2/12R^2)c^2/(b^2 + 2\nu bc + c^2)$ which will be maximized when the ratio $c/b = -1/\nu$. One concludes then that the maximum size of our hypothetical term $Eh^3(v^{\cdot} + w)^2/24(1-\nu^2)R^4$ must be less than $h^2/12R^2(1-\nu^2)$ multiplied by all the terms in Eq. (1) and is therefore negligible.

For establishing the negligibility of a term involving a product such as $[Eh^3/24(1-\nu^2)R^4]u'(w^{\cdot\cdot} - v^{\cdot})$ where terms from both lines 1 and 2 must be included in the comparison, a pyramiding technique is used. In this case a ratio of the type

$$(h^2/12R^2)be/[b^2 + 2\nu bc + c^2 + (h^2/R^2)(d^2 + 2\nu de + e^2)]$$

must be maximized but only after the two groups of terms in the denominator have been minimized relative to b or e independently.

Following similar reasoning, Koiter has suggested the addition of one more line of terms of the type in line 2 which, when compared to the sum of the lines 1 and 2, must in sum

Received June 8, 1971. The concept reported here is due to Koiter and was related to the author during the latter's tenure at the Technische Hogeschool, Delft, in the academic year 1966–1967.

* Associate Professor of Civil Engineering.